*Desalination and Water Treatment*
www.deswater.com
doi: 10.5004/dwt.2021.26641

212 (2021) 87–102
February

# Optimizing hybrid microbial fuel cell (MFC) and aerobic digestion reactor to gain simultaneous electricity generation and effective sludge digestion: an experimental study, mathematical modeling and recent achievements

Hadi Rasouli Sadabad[a], Gagik Badalians Gholikandi[b,*], Habibollah Arasteh Rad[c], Hamed Rasouli Sadabad[d]

[a]*Faculty of Mechanics, Electrical Power and Computer, Science and Research Branch, Daneshgah Blvd, Simon Bulivar Blvd, Tehran, Iran, email: rasouli.hadi@srbiau.ac.ir*
[b]*Faculty of Civil, Water and Environmental Engineering, Shahid Beheshti University, Hakimiye, Tehranpars, Tehran, Iran, emails: g.badalians@yahoo.com (G.B. Gholikandi), ha_rasouli@sbu.ac.ir (H.R. Sadabad)*
[c]*Department of Complex Dynamics Modeling, Institute of applied Intelligent Systems, University of Tehran, Tehran, Iran, email: habib.arasteh@ut.ac.ir*

Received 29 December 2019; Accepted 29 September 2020

**ABSTRACT**

Hybrid technologies have fascinated elevating attention globally. In this study, a microbial fuel cell (MFC) and an aerobic sludge digestion reactor have been combined to each other with the aim of generating direct electricity from municipal wastewater sludge simultaneous with its aerobic digestion. The optimal conditions for operational parameters of the processes have been determined using response surface methodology (RSM). The performances of both digestion and electricity generation process have been investigated comprehensively and the validity of the models have been evaluated by experimental investigations. According to the results, the optimal conditions for the merging MFC performance are 35.87°C ± 2°C, 7.27 ± 0.5, and 53.08% ± 2% for temperature, pH value of the cathode chamber, and the primary sludge content of the influent, respectively. In these conditions, the MFC is able to remove about 45.81% ± 2% of the volatile suspended solid (VSS) content of the feed sludge and generate 8,950 ± 50 mW/m$^3$ electrical power density.

*Keywords:* Optimization; Response surface methodology (RSM); Sludge management; Electricity generation; Aerobic stabilization

## 1. Introduction

Attention to environmental issues has been gradually increased in recent decades considering economic, ecological, and social responsibilities in order to reduce the impacts on the environment [1,2]. In this regard, endeavors have been concentrated on concepts like the circular economy which considers three principles, that is, to reduce, to reuse, and to recycle [1–5]. Therefore, considering the perspective of circular economy and environmental management concepts on waste materials, studies are carrying out to convert the potential energy of waste matters into useful forms of energy like electricity simultaneous with their digestion or disposal operations [6–12].

Also, increasing concerns about the environmental contamination by the discharge of the continuously growing amounts of waste materials (like sewage sludge) into the environment has accelerated investigations to control the

* Corresponding author.

1944-3994/1944-3986 © 2021 Desalination Publications. All rights reserved.

side effects of these waste products and simultaneously, reuse them [13–15]. As mentioned before, sewage sludge is one of the main waste materials which is generated during conventional wastewater treatment processes in significant quantities daily and contains noticeable amounts of organic and inorganic contaminants [16,17]. Normally, there are several energy generation methods from sewage sludge, relating to various digestion and/or stabilization processes [18–20]. Conversion of the potential biochemical energy of waste materials like sewage sludge directly to electricity via the catalytic reactions of bio-electrochemical microorganisms is another approach of generating bioenergy which has been attracted the attentions, recently. Generating electricity in these systems is carried out by microorganisms through various steps [18,21–29].

Regardless numerous studies, carried out on generating direct electricity from biomaterials, there is not categorized reliable data about the effect of operational parameters in cases on the performance of these systems. Furthermore, the performed assessments are carried out in different situations, resulted a noticeable variation in the reported results for parameters in each situation. Thus, the determination of the effect of operational conditions on the performance of bioelectrical systems in order to design industrial plants using the available different data is considerably complicated. Also, they have investigated only the primary and/or secondary sludge or their mixture as the reactor influent without evaluating the ratio of primary and secondary sludge in the mixture. According to carried out studies on the energy content of unknown organics in municipal wastewater streams, 66% of the energy entering the plant is captured in the primary sludge and the primary sludge had a higher energy content of energy than secondary and anaerobically digested sludge [24,30]. According to the exclusive characteristics of merging microbial fuel cell (MFCs), circular economy, and hybrid systems, in this study, the process of producing electricity, directly from municipal wastewater sludge (which contains both primary and secondary sludge) has been investigated during its aerobic digestion and the operational parameters of the processes have been optimized. In our previous studies [14–16], we have evaluated the performance of a two-chambered MFC and tried to optimize its behavior in various temperatures and pH values (as operational parameters) by response surface methodology (RSM) and artificial neural network (ANN). In the actual conditions, the sewage sludge in the wastewater treatment plants contains both primary and secondary sludge (mixed with each other), the recently done studies have not investigated the effect of their ratio in the mixed sludge on the electricity generation performance of MFCs or the digestion process in the digesters. Thus, in this study, we added the ratio of primary sludge to secondary sludge (PS/TS) as another determining operational parameter. Considering the results of our previous evaluations, the active microorganisms in the studied system are mesophilic aerobic bacteria and the amount of the primary sludge in the feed of the MFC is imperative in its performance in removing volatile suspended solid (VSS) as well as generating electricity. Therefore, due the noticeable differences between primary and secondary sludge chemical and microbial characterizations, we have considered the amount of the primary sludge in the sewage sludge composition integrated with other operational parameters like pH and the temperature.

In order to optimize the results of the study, RSM has been used to develop a mathematical correlation between operational parameters of the MFC and the generated electrical power density and the VSS removal efficiency as its responses. RSM is a reliable method in order to design experiments, evaluate the relationship between independent variables and responses individually as well as their interaction with each other. Moreover, it is able to optimize the process conditions with a defined amount of experiments, statistically [31–37].

## 2. Materials and methods

### 2.1. Sewage sludge collection, experimental setup, and chemicals

The primary and secondary sludge samples were collected from Tehran southern municipal wastewater treatment plant which treats 450,000 $m^3$ $d^{-1}$ municipal wastewater (Tehran, Iran). Table 1 represents the properties of the studied primary and secondary sludges.

Considering the huge amount of this plant's influence and the variations of the wastewater quality during the day and nights, we benefitted hybrid samples which were prepared from about 12 sampling process per 24 h. The quality of each hybrid sample was determined before each test and prior to inserting into the chambers of the MFC. The sludge samples were blended to be homogenous-enough prior to being charged into the chambers of the MFC. All of the experiments, pilot studies, data collection, and investigations were performed in a laboratory scale, two-chamber MFC. Fig. 1 represents the schematic view of the utilized MFC setup as well as the reactions of its different parts. According to Fig. 1, MFC has been formed from anode and cathode chambers, connected to each other by a proton exchange membrane (PEM) (Nafion TM 117, Dupont Co., USA). The volume of chambers was about 2,500 mL and the net volume of them adjusted to 2,000 mL. The chambers contained three graphite electrodes

Table 1
Characterizations of the utilized primary and secondary sludge

| Item | pH | Temperature (°C) | Total COD[a] | VSS[b] (mg/L) | TSS[c] (mg/L) |
|---|---|---|---|---|---|
| Primary sludge | 6–7.2 | 18–25 | 9,500–15,500 | 7,200–9,000 | 10,000–14,500 |
| Secondary sludge | 6.5–7.5 | 18–25 | 6,500–11,400 | 4,500–5,500 | 6,200–8,900 |

[a]Chemical oxygen demand; [b]Volatile suspended solids; [c]Total suspended solids.

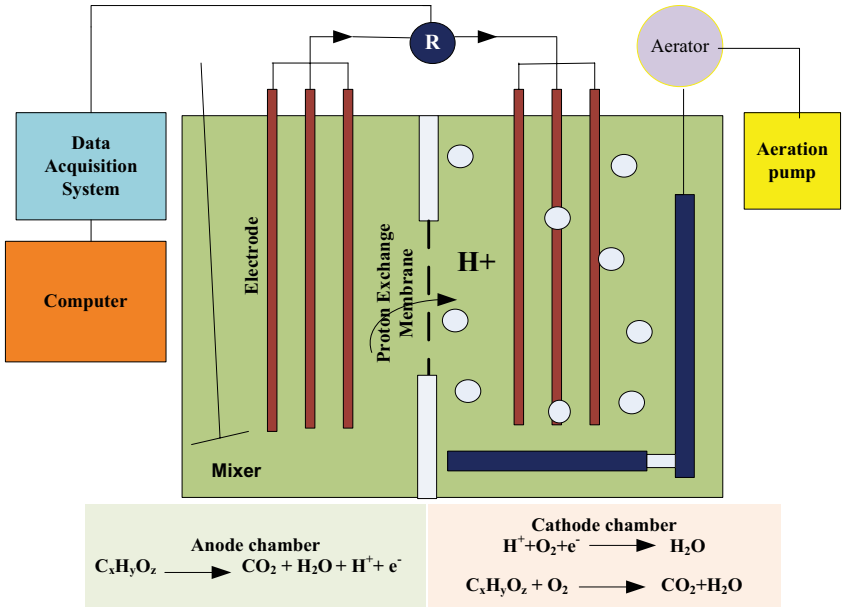



Fig. 1. Utilized microbial fuel cell (MFC) and the anodic and cathodic reactions in its chambers [14].

which were fixed 30 mm apart from each other. The length, width, and thickness of the electrodes were equal to 200, 40, and 1 mm, respectively. One aerator has been fixed in the bottom of the cathode chamber and another one has been placed longitudinally parallel to its electrodes with the same height. Also, a magnetic bar has been used to mix the content of the anode chamber. In order to keep the volume of the mixed liquid in the reactor unchanged, deionized water was supplied at times to compensate for the volatilized water by mixing or aeration. The electrodes in both chambers were connected to each other as well as an external resistance ($R$) using copper wire. Each run of the experiments took long about 120 h (5 d). A precision multimeter has been utilized (2,700, Keithley, OH, USA) with a voltage across resistor recorded every 30 min intervals and a data acquisition system connected to a computer. The determination of VSS carried out on the prepared sample, containing equal parts of the samples obtained from the bottom, middle, and top of each chamber. The experiments were conducted according to the American Public Health Association [38].

All of the chemicals, used in this study have been provided by Merck® Co., Germany. The pH adjustments in both chambers have been performed by sulfuric acid ($H_2SO_4$, 98%, 0.3 M) and caustic soda (NaOH; 0.5 M). The temperature of the reactor has been set on the designed values by a ventilated heating/cooling cabin. At the initial point, acetate, and glucose were entered over the sludge in the anode chamber to help the bio-electrochemically activated microbial community to prevail. The amounts of acetate and glucose were about 1.5% and 3% the VSS of the influent sludge, respectively. The VSS removal efficiency of the process has been evaluated in various operational conditions, to represent the aerobic digestion process. Also, the generated electricity was controlled using the measured voltage and the current density. This data used to calculate the generated electrical power density. Eqs. (1) and (2) show the relations that have been used for calculation of the VSS removal efficiency [39] and the generated electrical power density [40], respectively.

$$\text{VSS Removal Efficiency, \%} = \left[\frac{\left(\text{VSS}_{(\text{raw sludge})} - \text{VSS}_{(\text{treated sludge})}\right)}{\text{VSS}_{(\text{raw sludge})}}\right] \times 100 \quad (1)$$

$$P = \frac{V \times \text{I}}{V_a} \times 1{,}000 \quad (2)$$

In Eq. (2) $P$ is the power density (W/m$^3$), $V$ is the measured voltage of the process, $I$ is the current density (mA/m$^2$), and $V_a$ is the net volume of the liquid in the anode (m$^3$). Implementation of the process in various operational situations was controlled under open circuit conditions (OCP). Polarization curves were established by determining the voltages obtained with different external resistors (10–1,500 Ohms) after the voltage stabilizing. Also, in order to obtain polarization curves, linear sweeping voltammetry (LSV) analysis has been used with the employed scan rate of 0.1 mV/S from the anode open circuit potential (OCP) to the minimum cell potential. In order to keep the effect of the DO on the cathodic chamber's process constant, he tried to keep the concentration of the dissolved $O_2$ close to the saturation level during the process using aerators in this chamber.

### 2.2. Experimental design and data analysis

RSM is a practical technique in outreach, performance optimization, and design improvement of new processes and product formulations. The central composite design (CCD) which is introduced first by Box and Wilson in 1951,

is an effective design method for sequential experimentation [37]. The responses are related to the selected parameters by linear or quadratic models in the optimization process. Eq. (3) demonstrates a quadratic model, which also includes the linear model [14]:

$$z = x_0 + \sum_{j=1}^{K}\left(x_j y_j\right) + \sum_{j=1}^{K}\left(x_{jj} y_j^2\right) + \sum_{i=1}^{k-1}\sum_{j=i+1}^{K}\left(x_{ij} y_i y_j\right) + e_i \quad (3)$$

where $z$ demonstrates the response, $y_i$ and $y_j$, variables ($i$ = 1–$k$), $x_0$, the constant coefficient, $x_j$, $x_{jj}$, and $x_{ij}$ ($i$ and $j$ = 1–$k$), interaction coefficients of linear, quadratic, and the second-order terms, respectively, $k$, the number of independent parameters and finally, $e_i$, the error.

In this study, the CCD with three factors was applied by Design Expert 10.0. The independent variables and their ranges and levels have been shown in Table 2. These parameters have been chosen because of their noticeable influences on electricity generation and aerobic digestion processes [41–45].

The ranges and levels have been determined considering the results of the preliminary experiments and the reported results by literature [19,42–47]. Experimental conditions of CCD runs of Design Expert 10.0 and its corresponding responses have been demonstrated in Table 3.

First five columns of Table 3 show runs order (considering standard deviation) and the experimental conditions, determined by the CCD. The last two columns represent the VSS removal efficiency and the generated electrical power density as process outputs. All the experiments were done in triplicate and the results eventuated from replicate analyses. The values reported for the VSS removal efficiency are the average of both chambers of the MFC. Also, the values of the generated electrical power density are the peak value of the recorded data from the initiating point of each run till its finishing.

Table 2
Levels and ranges of the Independent variables for the CCD experiment

| Variables | Ranges and levels | | | | |
|---|---|---|---|---|---|
| | –2 | –1 | 0 | 1 | 2 |
| Temperature, °C | 5 | 20 | 35 | 50 | 65 |
| pH | 3 | 5 | 7 | 9 | 11 |
| PS/TS, % | 100 | 75 | 50 | 25 | 0 |

## 3. Results and discussion

### 3.1. Experimental results evaluation by Design Expert

As previously mentioned, in order to evaluate the interactive impacts of operational parameters on responses, experiments were carried out under various operational conditions, designed by CCD method. If the achieved ratio of the maximum value of the proposed functions to their minimum is more than 10, the approximation obtained by these

Table 3
Experimental conditions of central composite design (CCD) runs of Design Expert and the corresponding responses

| | | Factor 1 | Factor 2 | Factor 3 | Response 1 | Response 2 |
|---|---|---|---|---|---|---|
| Std | Run | *A*: Temperature, °C | *B*: pH | *C*: PS/TS[a], % | VSS removal efficiency, % | Power density, mW/m$^3$ |
| 6 | 1 | 35 | 7 | 100 | 39.83 | 7,000.74 |
| 7 | 2 | 65 | 7 | 50 | 10.13 | 592.8 |
| 1 | 3 | 17.2 | 9.4 | 20.3 | 22.87 | 1,418.29 |
| 14 | 4 | 35 | 7 | 50 | 46.66 | 6,289.13 |
| 9 | 5 | 35 | 11 | 50 | 24.98 | 3,019.82 |
| 10 | 6 | 52.8 | 9.4 | 20.3 | 24.71 | 1,801.28 |
| 4 | 7 | 52.8 | 4.6 | 20.3 | 19.87 | 1,951.79 |
| 19 | 8 | 17.2 | 4.6 | 16.4 | 16.38 | 1,321.82 |
| 18 | 9 | 35 | 7 | 50 | 51.68 | 4,601.21 |
| 11 | 10 | 35 | 7 | 20.3 | 43.36 | 6,293.12 |
| 17 | 11 | 17.2 | 4.6 | 50 | 22.14 | 987.05 |
| 13 | 12 | 35 | 7 | 20.3 | 46.39 | 6,292.32 |
| 2 | 13 | 35 | 7 | 50 | 46.42 | 6,287.04 |
| 20 | 14 | 35 | 7 | 50 | 46.33 | 6,290.17 |
| 5 | 15 | 5 | 7 | 50 | 3.93 | 302.89 |
| 12 | 16 | 52.8 | 9.4 | 79.7 | 18.39 | 1,596.14 |
| 16 | 17 | 52.8 | 4.6 | 79.7 | 18.03 | 3,021.33 |
| 15 | 18 | 35 | 3 | 50 | 4.13 | 371.86 |
| 8 | 19 | 35 | 7 | 50 | 46.17 | 6,301.10 |
| 3 | 20 | 17.2 | 9.4 | 79.7 | 16.76 | 1,981.31 |

[a]TS = PS + SS

functions will be accurate to predict the system's behavior [14,36]. Regarding Table 3, the range of the objective functions responses are from 3.93 to 51.68 for the VSS removal efficiency and 302.89 to 7,000.74 for the generated electrical power density. These values generate 13.15 and 23.12 as the maximum to the minimum ratio for the responses which are more than 10. So, all attainable transformations were tried in the program to enhance the model's prediction ability. The VSS removal efficiency and the generated electrical power density data were fitted to two quadratic models.

Closer values of $R^2$ to 1 ensure a sufficient correlation between the data derived from the experiment and the model [32]. In this study, the considerably high values of the adjustment coefficients of the models ($R^2_{adj}$ = 0.9530 and 0.9185 for the VSS removal efficiency and the generated electrical power density, respectively), proved that the models are appropriate to describe the relation of operational conditions and responses with high precision. Table 4 shows the ANOVA test results for the proposed model of VSS removal efficiency. Also, Table 5 demonstrates this data for the generated electrical power density of the reactor. As demonstrated by the tables, *p*-values of the models were determined less than 0.0001 for the VSS removal efficiency and the generated electrical power density, respectively. This value is remarkably lower than the desired limit (0.05) and confirms that these models are remarkably reliable in being utilized for prediction of the process behavior in different operational conditions.

According to the results of the optimization process in Design Expert software, the items that marked by "*" in Tables 4 and 5 have a negligible role in the final approximation equations. The noticeably low values of their coefficients in the final equations prove this fact. The resulted quadratic approximation functions from the models for the VSS removal efficiency and the generated electrical power density are shown in Eqs. (4) and (5).

$$\begin{aligned}\left(\text{VSS removal efficiency}\right)^{1.11} &= -181.210 + \left(4.772 \times \text{Temperature}\right) + \left(46.998 \times \text{pH}\right) - \left(0.0321 \times \left(\text{PS/TS}\right)\right) + \\ &\left(0.018 \times \text{Temperature} \times \text{pH}\right) + \left(1.420 \times \text{Temperature} \times \left(\text{PS/TS}\right)\right) - \left(0.014 \times \text{pH} \times \left(\text{PS/TS}\right)\right) - \\ &\left(0.070 \times \left(\text{Temperature}\right)^2\right) - \left(3.216 \times \left(\text{pH}\right)^2\right) - \left(\left(7.678E-4\right) \times \left(\text{PS/TS}\right)^2\right)\end{aligned} \tag{4}$$

$$\begin{aligned}\left(\text{Electrical power density}\right)^{0.63} &= -707.512 + \left(19.000 \times \text{Temperature}\right) + \left(154.637 \times \left(\text{pH}\right)\right) + \left(1.736 \times \left(\text{PS/TS}\right)\right) - \\ &\left(0.306 \times \text{Temperature} \times \text{pH}\right) - \left(\left(2.12\text{E}-3\right) \times \text{Temperature} \times \text{PS/TS}\right) - \left(0.068 \times \text{pH} \times \text{PS} / \text{TS}\right) - \left(0.230 \times \text{Temperature}^2\right) - \\ &\left(9.637 \times \text{pH}^2\right) - \left(\left(7.637E-3\right) \times \left(\text{PS/TS}\right)^2\right)\end{aligned} \tag{5}$$

The positive signs in front of the terms indicate synergistic and the negative signs show antagonistic effects in the equations. Overall, regarding Table 3, Eqs. (4) and (5), the VSS removal efficiency and the generated electrical power density at designed experimental conditions can be predicted by the models. Fig. 2 shows the comparison of the response values obtained from prediction and experiments.

Table 4
ANOVA test results for the VSS removal efficiency

| Response: 1 | Transform: power | | | Lambda: 1.11 | | Constant: 0 |
|---|---|---|---|---|---|---|
| Source | Sum of squares | df | Mean square | *F*-value | *p*-value (Prob. > *F*) | Clarification |
| Model | 11,584.23 | 9 | 1,287.14 | 43.79 | <0.0001 | Significant |
| *A*-Temperature | 26.61 | 1 | 26.61 | 0.91 | 0.3638[a] | – |
| *B*-pH | 273.78 | 1 | 273.78 | 9.32 | 0.0122 | – |
| *C*-PS/TS | 301.64 | 1 | 301.64 | 10.26 | 0.0094 | – |
| *AB* | 4.47 | 1 | 4.47 | 0.15 | 0.7048[a] | – |
| *AC* | 4.54 | 1 | 4.54 | 0.15 | 0.7027[a] | – |
| *BC* | 7.97 | 1 | 7.97 | 0.27 | 0.6138[a] | – |
| $A^2$ | 7,115.59 | 1 | 7,115.59 | 242.10 | <0.0001 | – |
| $B^2$ | 4,770.18 | 1 | 4,770.18 | 162.30 | <0.0001 | – |
| $C^2$ | 6.64 | 1 | 6.64 | 0.23 | 0.6448[a] | – |
| Residual | 293.91 | 10 | 29.39 | – | – | – |
| Lack of fit | 271.73 | 5 | 54.35 | 12.25 | 0.0078 | – |
| Pure error | 22.18 | 5 | 4.44 | – | – | – |
| Cor. total | 11,878.14 | 19 | – | – | – | – |

[a]Negligible effect on the model equation.

Table 5
ANOVA test results for the generated electrical power density

| Response: 2 | Transform: power | | Lambda: 0.63 | | Constant: 0 | |
|---|---|---|---|---|---|---|
| Source | Sum of squares | df | Mean square | *F*-value | Prob. > *F* | Clarification |
| Model | 1.173E+005 | 9 | 13,028.44 | 24.81 | <0.0001 | significant |
| *A*-Temperature | 1,383.57 | 1 | 1,383.57 | 2.63 | 0.1356[a] | – |
| *B*-pH | 2,402.70 | 1 | 2,402.70 | 4.57 | 0.0581 | – |
| *C*-PS/TS | 2,136.85 | 1 | 2,136.85 | 4.07 | 0.0713 | – |
| *AB* | 1,352.86 | 1 | 1,352.86 | 2.58 | 0.1396[a] | – |
| *AC* | 10.11 | 1 | 10.11 | 0.019 | 0.8924[a] | – |
| *BC* | 186.31 | 1 | 186.31 | 0.35 | 0.5647[a] | – |
| $A^2$ | 76,939.90 | 1 | 76,939.90 | 146.50 | <0.0001 | – |
| $B^2$ | 42,830.12 | 1 | 42,830.12 | 81.55 | <0.0001 | – |
| $C^2$ | 656.68 | 1 | 656.68 | 1.25 | 0.2896[a] | – |
| Residual | 5,251.89 | 10 | 525.19 | – | | – |
| Lack of fit | 5,251.82 | 5 | 1,050.36 | 71,262.52 | <0.0001 | – |
| Pure error | 0.074 | 5 | 0.015 | – | – | – |
| Cor. total | 1.225E+005 | 19 | – | – | – | – |

[a]Negligible effect on the model equation.

According to Figs. 2a and b, the experimental data have been scattered symmetrically around the predicted data near to them which means actual and predicted data are compatible with the responses. It means these models are appropriate enough to estimate the VSS removal efficiency as well as the generated electrical power density of the process in various operational conditions.

### *3.2. Response surface plotting and impacts of operational parameters at optimum conditions*

Figs. 3 and 4 illustrate the variations of the responses by changing the operational parameters in surface plots. These plots have been graphed using Eqs. (4) and (5). The surface plots demonstrate the impacts of two operational parameters on the response at the central point of the third one.

As shown in Fig. 3a, the VSS removal efficiency of the process shows modification by elevating temperature from the lower values to about 35°C and gets its climax at this point. Simultaneously, by increasing pH values from 3, the VSS removal efficiency of the reactor demonstrates an improving trend and keeps this state till 7. But, by increasing both the temperature and the pH values to higher than 35°C and 7°C, respectively, the VSS removal efficiency demonstrates a downward trend. These observations are highly compatible with previous studies [14,19]. Also, according to Figs. 3b and c, the VSS removal efficiency shows variations by changing the primary sludge content of the influent and decreases by its increase. Also, the dependency of the VSS removal efficiency to the primary sludge content of the influent sludge is less than other operational parameters (temperature and pH).

Fig. 4 illustrates the relation of the operational parameters and the VSS removal efficiency of the process in contour plots.

According to Fig. 4a, the best operation conditions of the process are related to the central part of the contour plot which is between an expanded temperature range of about 25°C–45°C and pH values from approximately 6 to about 9 (when the PS/TS is about 0.5). At the extreme parts of temperature and pH ranges the value of the response is considerably low. Also, Figs. 4b and c show that the higher values of the VSS removal efficiency have been observed in the lower PS/TS values. In other words, increasing the primary sludge content of the reactor feed decreases its ability to remove the VSS. Another important point is that in the extreme values of pH or temperature, the dependency of the response to the PS/TS ratio is considerably low, and it does not show remarkable changes in these ranges of the operational parameters.

According to this fact that the VSS removal efficiency represents the performance of the aerobic stabilization process of the reactor, it seems that in very high and low values of temperature and pH, the microorganisms are not able to work regularly and as a result, they cannot remove the VSS of the influent, even if primary, or secondary sludge [14,42,48].

Figs. 6 and 7 show the surface and the contour plots as an estimate of the generated electrical power density in various operational conditions. These figures are graphical representations of Eq. (5).

Fig. 5a shows the variations of the generated electrical power density in different temperatures and pH values. According to the Fig. 5, increasing the temperature from very low to medium temperatures modifies the generated power density as well as changing pH values from acidic to neutral conditions. By increasing temperature and pH to higher than 35°C and 7°C, respectively, the values of the generated electrical power density show decrease. These observations are compatible with the previous studies [14,44,49,50]. These trends are similar to the results, shown

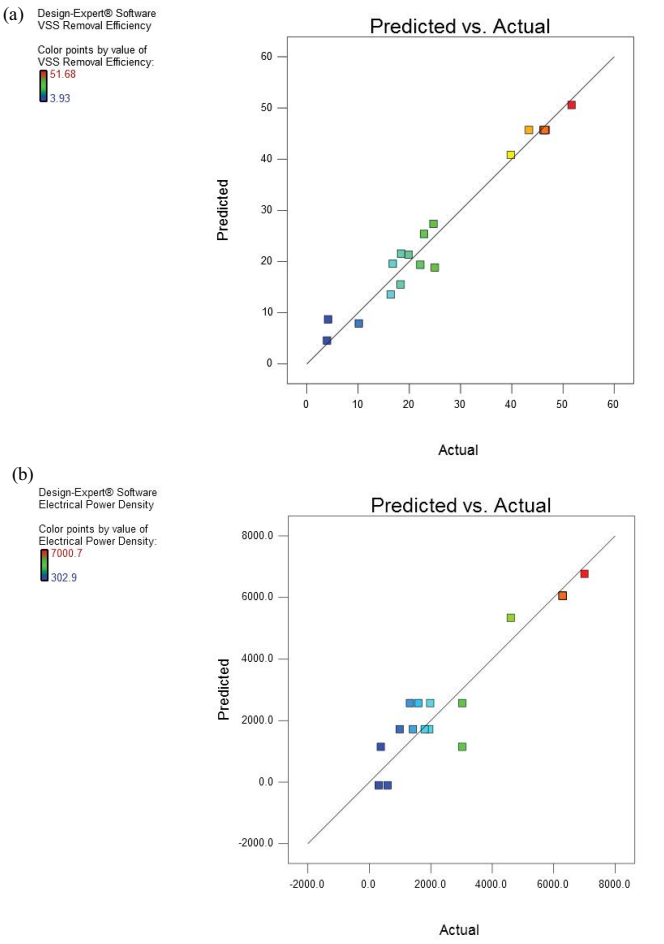



Fig. 2. Comparison of predicted and actual values; (a) the VSS removal efficiency and (b) the generated electrical power density.

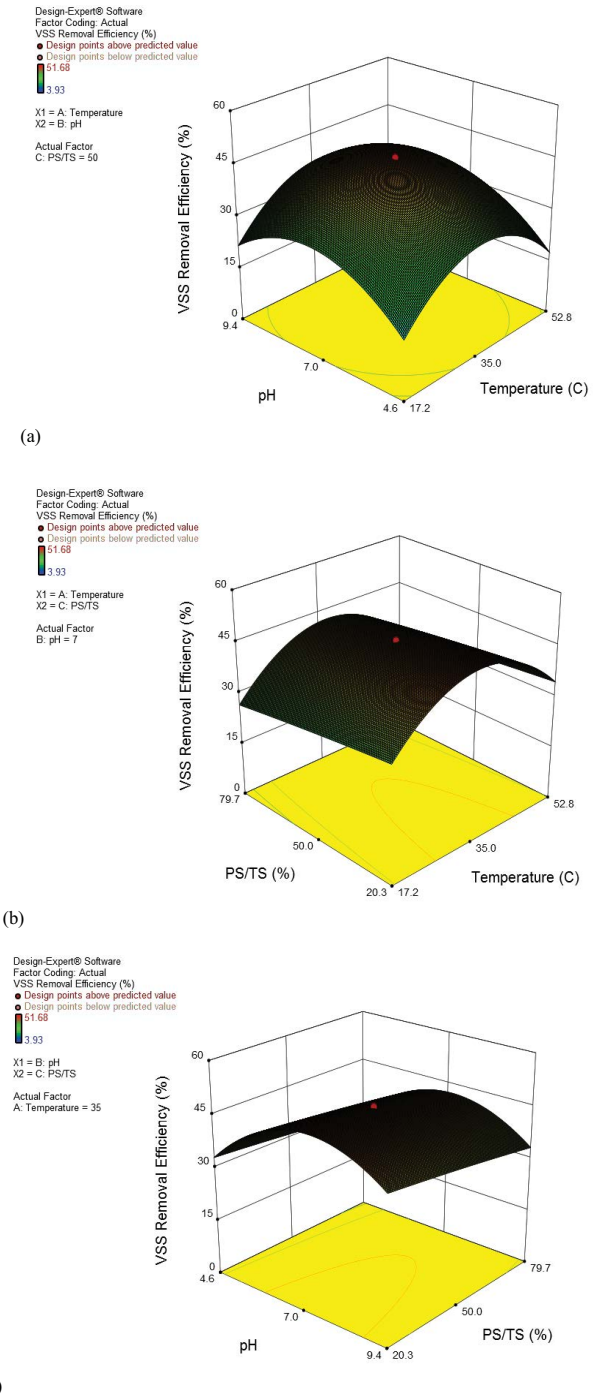
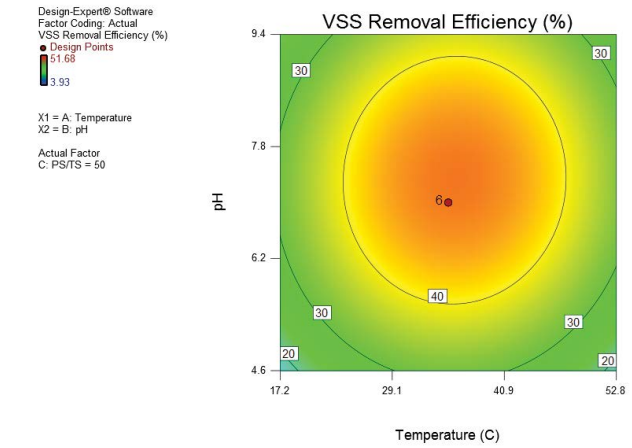



Fig. 3. Surface plot of the VSS removal efficiency at various (a) temperatures and pH values, (b) temperatures and PS/TS ratios, and (c) PS/TS ratios and pH values.

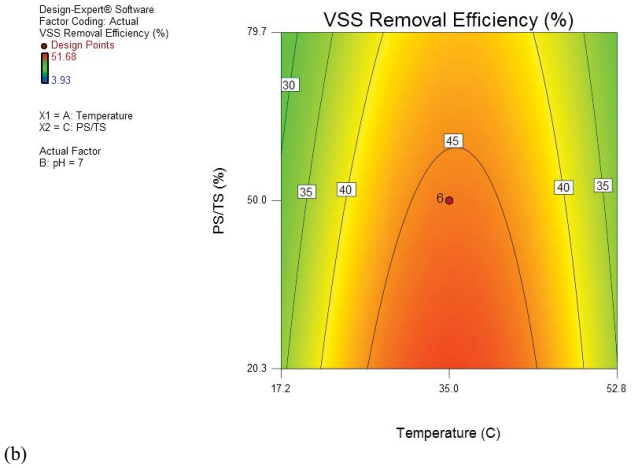
in Figs. 5b and c, too. Despite the VSS removal efficiency, increasing the PS/TS ratio in the reactor feed modifies the generated electrical power density in all pH values and temperatures, as shown in Figs. 5b and c. The contour plots have been developed the generated electrical power density as a function pH and/or temperature and/or PS/TS ratios.

According to Fig. 6a, the generated electrical power density attains a peak in the range of 6–8.5 for pH and 20°C–45°C for temperature (at PS/TS ratio equal to 0.5). Also, growing the generated electrical power density has been observed by increasing PS/TS ratio in the reactor feed increases. In other words, raising the primary sludge content of the reactors feed decreases the VSS removal efficiency, but modifies the electricity generation process in the reactor. This observation is proved by recent studies [19,24,51]. It seems that the higher amounts of the produced electricity from effluents that contain higher ratios of primary sludge is because of the remarkably higher content of easily biodegradable compounds of the primary sludge [51].

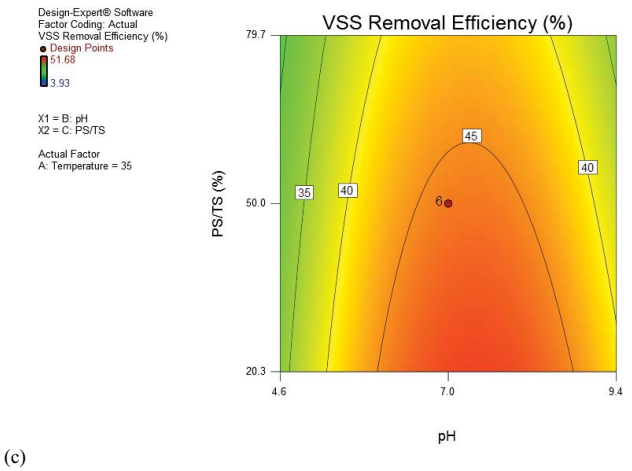
Also, according to the aerobic nature of the digestion process in the cathode chamber and dominantly biological processes in both chambers of the reactor, it is assumed that the temperature affects the process by changing the DO concentration of the substrate and the activities of the biological culture [14,15,52]. In other words, increasing the temperature improves the reaction rate and progress which uses oxygen for oxidation of the organics in sewage sludge during aerobic digestion, and thus, enhances the VSS removal efficiency. In temperatures higher than 45°C, the amount of DO in the solutions remarkably decreases and this reduction affects the removal efficiency of the processes




(a)

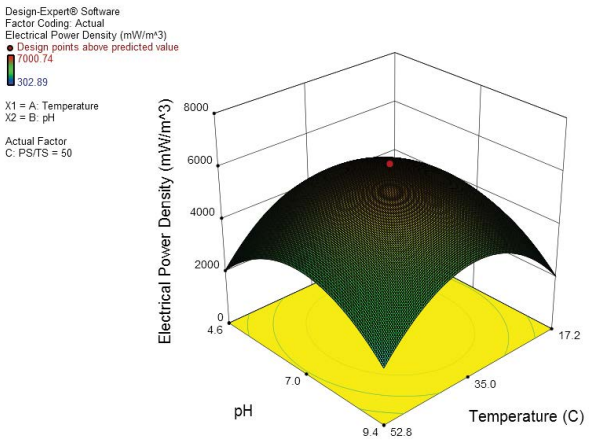



(b)

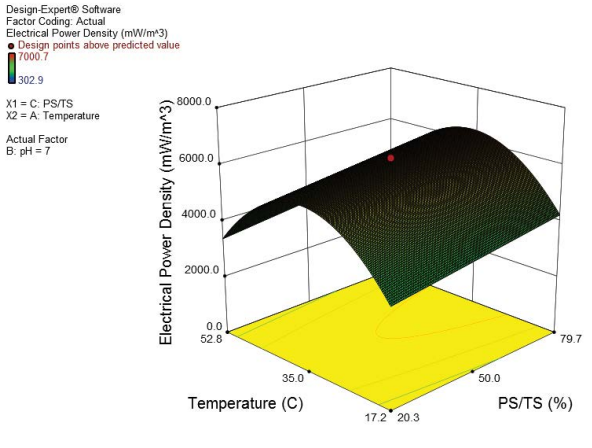



(c)

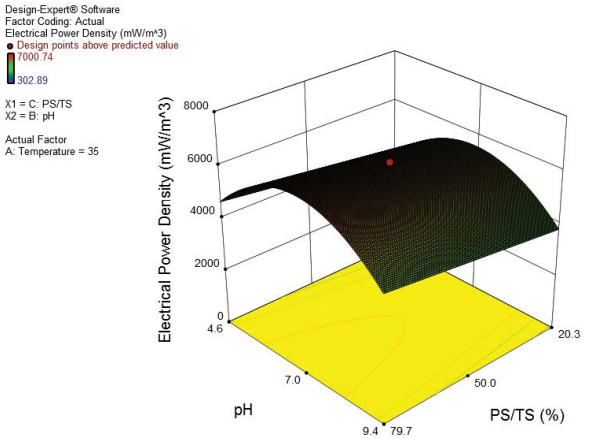
Fig. 4. Contour plots of the VSS removal efficiency at various (a) temperatures and pH values, (b) temperatures and PS/TS ratios, and (c) PS/TS ratios and pH values.




(a)




(b)




(c)

Fig. 5. Surface plots of the generated electrical power density at various (a) temperatures and pH values, (b) temperatures and PS/TS ratios, and (c) PS/TS ratios and pH values.

[52,53]. This pattern is correct for electricity-generating microorganisms, too [43,49,53–55]. Also, the variations of the responses by changing pH values seem to be related to hydrogen ions and carbon dioxide as well as ammonia as the products of the aerobic digestion process. Hydrogen ions and carbon dioxide tend to acidify the content of the chamber. The reduction of pH may take place when ammonia is oxidized to nitrate if the alkalinity of the wastewater is not enough to buffer the solution, too. In the extreme values of pH, it would be formidable for microorganisms and bacteria to generate these chemicals and advance the

process [39,56–58]. According to the literature, the reported reason for the variations in the electricity generation performance of the reactor is similar to the VSS removal efficiency. As mentioned before, the bacterial activities are well-known to be affected by temperature and pH, with biological processes as well as the composition of the feed sludge (due to the differences between primary and secondary sludge chemical and bacterial properties) [23,43,59]. Therefore, it is expected that the performance of the reactor would be affected by the variation of the mentioned operational conditions, due to its impacts on microorganisms' kinetics, the rates of oxygen reactions on the cathode, as well as the rate of mass transfer of protons through the liquid, especially in the cathode chamber. From this perspective, the efficiency of these processes in the cathode chamber affects the peak value of the generated electrical power densities in these systems [43,59–61]. Also, a wide variety of microorganisms not conveniently function in extremely high or low temperatures or pH values, due to their effect on critical parameters like $H^+$ and DO concentrations, integrated with the cathode material nature and its interaction with water. Moreover, the effect of pH on exchanging $H^+$ between chambers during the processes is an important parameter in the progress of the occurring processes. The effects of acidity on Nafion PEMs within MFCs have been considered in several studies [62–64]. Moreover, the internal resistance of the PEM membrane is increased in a considerably low concentration of $H^+$ ions (high pH values) compared with neutral and acidic conditions [62–65]. Also, considerably high concentrations of protons in very low pH values prevent generation of these ions, biologically [44]. Therefore in these conditions, the generated electrical power density is very lower comparing with the moderate conditions [65–69]. Also, the acceptable intervals of the operational conditions area for the VSS removal and the electricity generation processes are covering each other conveniently. This observation would be reasonable if the VSS is considered as a food and energy source for electrogenic bacteria. The variations of the operational parameters to normal temperatures and pH values increase the metabolic reactions of the microorganisms and enhance the performance and the efficiencies of the reactor [48,49,70–72]. Also, the actual content of the primary sludge of the sewage sludge in the wastewater treatment plants is between 40% and 50% which is covered by the model very well [23,44,46,73,74].

### 3.3. Experimental assessment results and the comparison of the experimental and the model results

In order to evaluate the accuracy of the model results, extra experiments have been designed and executed. In other words, the performances of the aerobic stabilization and electricity generation processes in various operational conditions have been investigated and compared with the model results. Fig. 7 shows the results of the experiments for the VSS removal efficiency of the reactor as represent of the aerobic stabilization process. As shown in the legends of the figures, the evaluations of the effect of temperature have been executed at pH values about 7 and PS/TS ratio of 0.5 in the reactor feed. Also, the effect of pH values has been evaluated at 35°C and PS/TS ratio of 0.5, and finally,

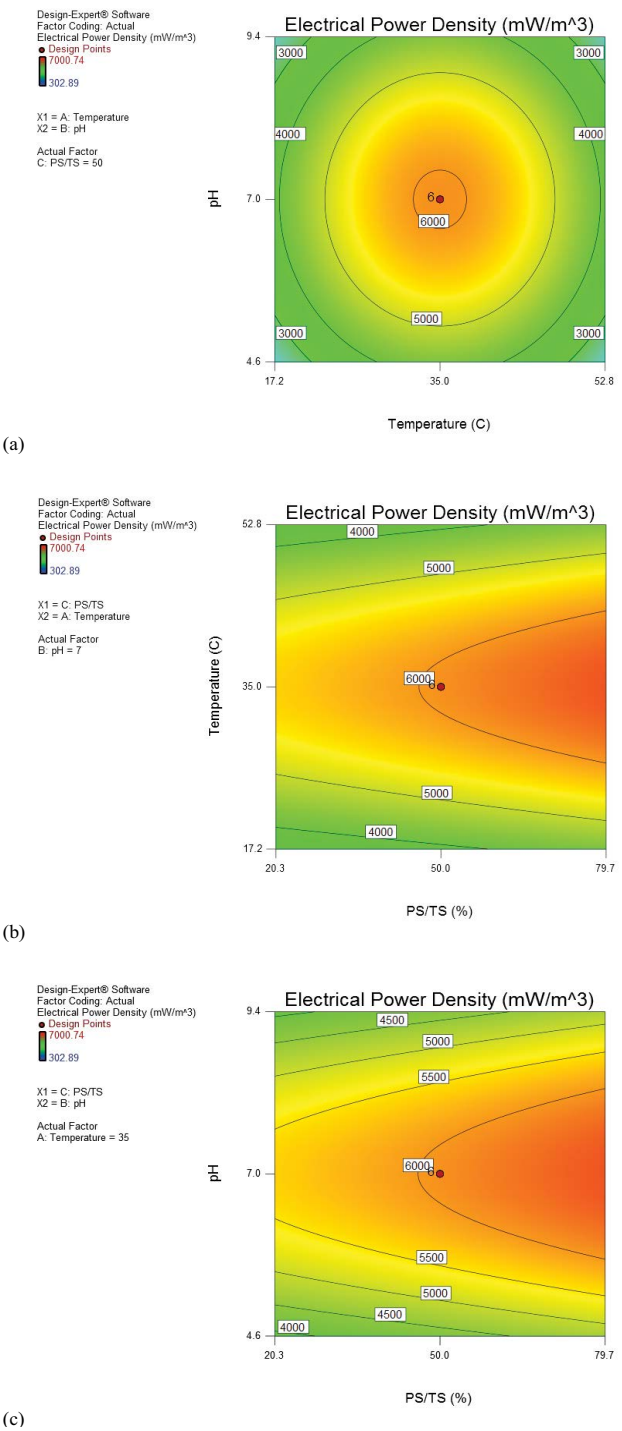



Fig. 6. Contour plot of the generated electrical power density at various (a) temperatures and pH values, (b) temperatures and PS/TS ratios, and (c) PS/TS ratios and pH values.

the effect of primary sludge content of reactor influent has been carried out at 35°C and neutral conditions (pH = 7).

According to Fig. 7, increasing pH value from acidic to neutral conditions modifies the VSS removal efficiency of the reactor. Also, the VSS removal efficiency shows upward trend by elevating temperature from 5°C to 40°C and then

downward trend in higher temperatures. This observation is highly compatible with the model results. Finally, as predicted by the model, increasing the primary sludge content in feed sludge of the reactor clearly reduces the VSS removal efficiency of the reactor. The VSS removal efficiency of the process smoothly decreases from 52% to 40% by increasing the primary sludge content of the reactor influent from 0 to 100%.

Also, the results of experiments for the parameters, related to the generated electricity, have been provided in Figs. 8 and 9. Fig. 8 shows the polarization curves of the process in various operational conditions and Fig. 9 represents the generated electrical power density in various values of the operational parameters. According to the legends of the figures, the evaluations of the effect of temperature have been executed at pH values about 7 and PS/TS ratio of 0.5 in the reactor feed. Also, the effect of pH values has been evaluated at 35°C and PS/TS ratio of 0.5, and finally, the effect of primary sludge content of reactor influent has been carried out at 35°C and neutral conditions (pH = 7), just like the evaluations of the VSS removal efficiency.

It can be seen in Fig. 8 that increasing the primary sludge content of the reactor feed boosts the generation of electrical power density, noticeably. In other words, by

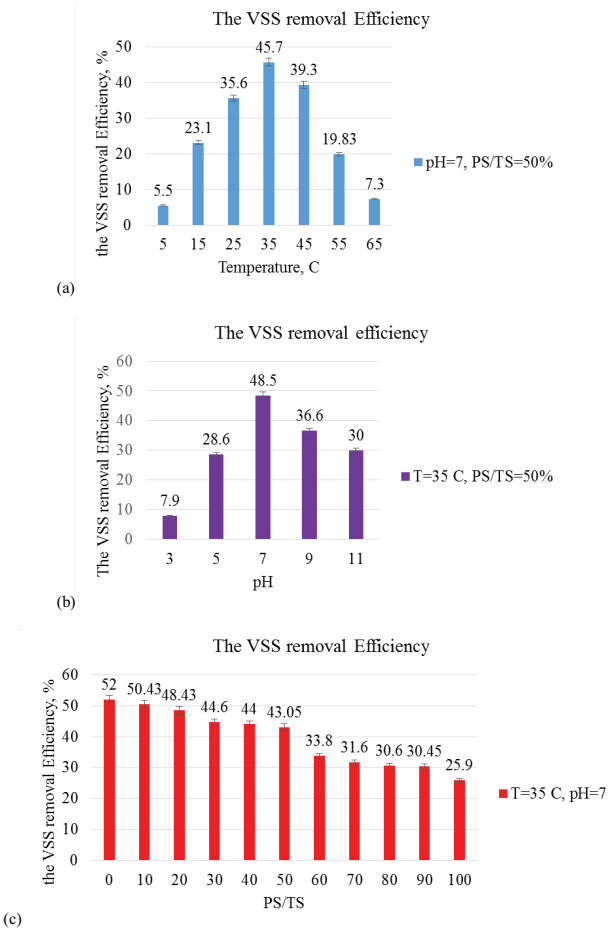
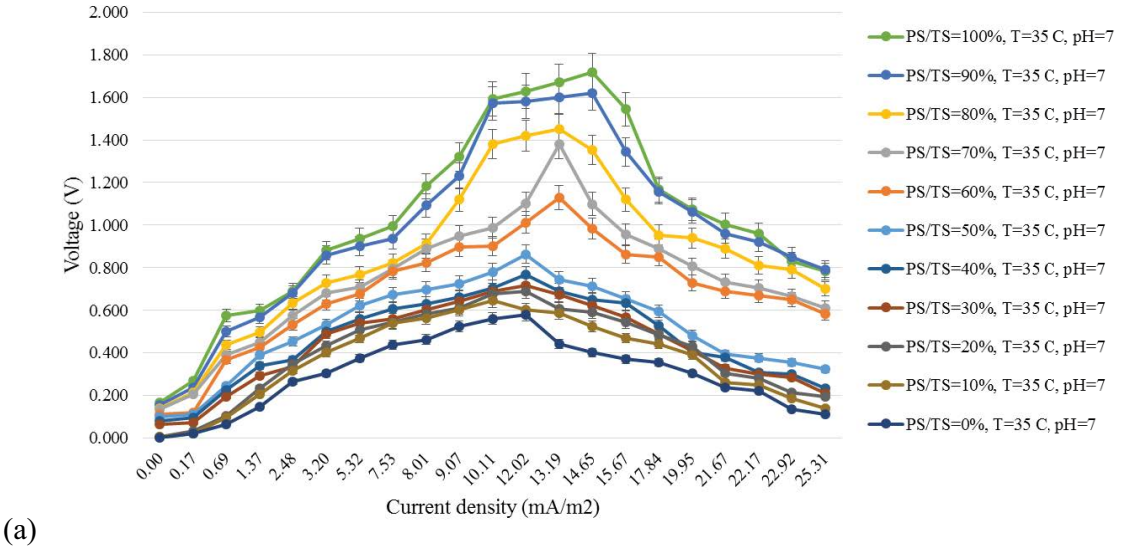


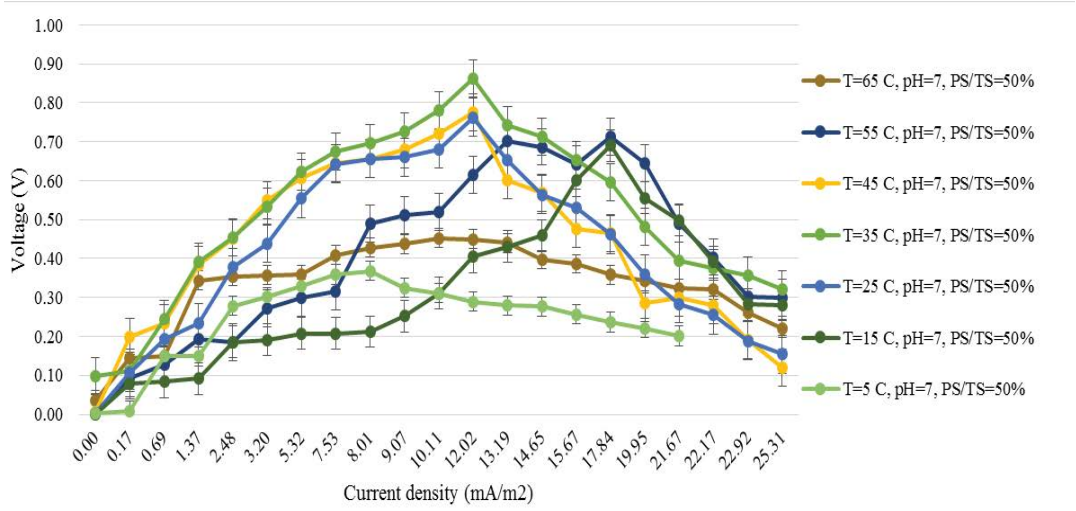

Fig. 7. VSS removal efficiency of the process at various, (a) temperatures, (b) pH values, and (c) PS/TS ratios.

increasing the PS/TS ratio in the reactor influent sludge, the current density, and especially voltage of the generated electricity demonstrate an evenly rising upward trend and finally, the maximum value of the voltage and the current density of the generated electricity have been observed when the primary sludge content of the influent is 100%. Also, the electricity generation process showed its best performance in mild temperatures and neutral conditions. As shown in Fig. 8b, the behavior of the process' polarization curves within 25°C–45°C temperature interval are nearly to each other. It means that the electricity generation behavior of the reactor in these operational conditions are considerably similar. Also, the maximum value of the generated voltages and the climax amount of the generated electrical current density are close and considerably more than lower and higher temperatures. This behavior is relatively similar with the changes in the pH values. The presented performance of the reactor for electricity generation in pH values from 5 to 9 are approximately close to each other but higher than more acidic or basic conditions.

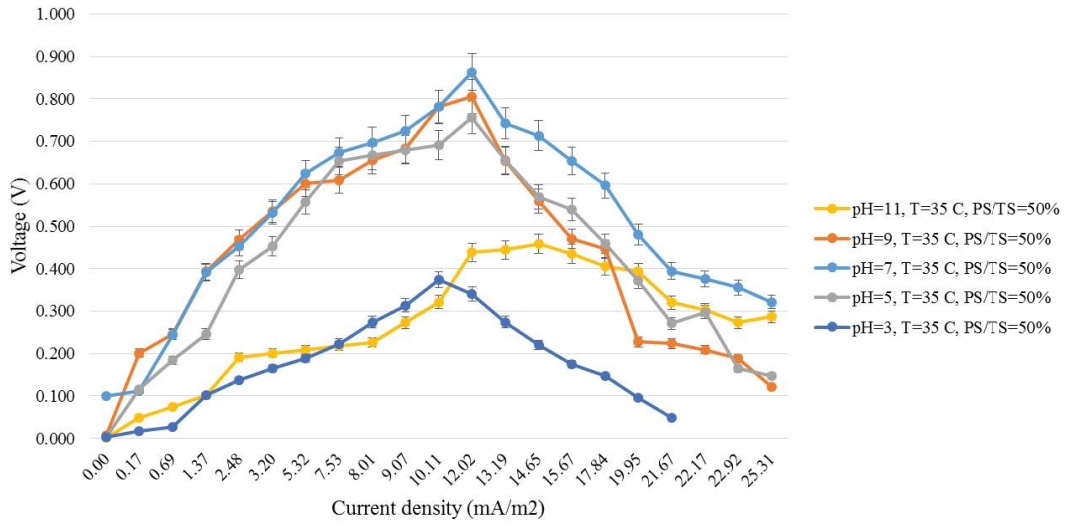
It is stated previously that the generated power density of MFC is highly dependent to the current density as well as the voltage. Thus, it demonstrates change by any fluctuation in the values of these parameters. According to Fig. 9a, as the PS/TS ratio increases in the feed sludge content, the value of the generated electrical power density increases in a smooth trend. At the starting point, the value of the produced power is noticeably low in all of the conditions, but the rate of its increase is remarkably higher in higher ratios of the PS/TS. Despite the uniform increase of the generated power density by raising the PS/TS ratio, by increasing the temperature from very low (5°C) to very high temperatures (65°C), the produced electrical power density revealed an upward and then downward trends as well as its performance change by variation of pH values (as shown in Figs. 9b and c). The MFC shoed its maximum amount of the generated electrical power density at 35°C and pH values near to 7. These observations are compatible with our recently done studies for waste-activated sludge [14]. Also, the results obtained from the experiments are highly compatible with the model results and the trends changes of the model responses are approximately the same with the experimental results. These trends can be justified considering the fact that at very high or very low temperatures and pH values, the electrogens are not able to work or grow conveniently, and as a subsequent, negatively influence running electricity generating processes in MFC's chambers which are majorly biological [14,15,65,69]. As mentioned before, elevation of the temperature boosts the activity of various bacteria cultures and microorganisms and decreases the internal resistance of the system against proton exchange significantly, and as a result modifies the VSS removal efficiency as well as the generated power density [14,45,60,69,75–78]. Moreover, because of the aerobic nature of the processes in the cathode chamber, this growth in biological activity increases the demand for dissolved oxygen in this chamber. On the other hand, increase in temperature causes a drop in the amount of available oxygen in the solutions [43,46,52]. The concentration of dissolved oxygen at temperatures higher than 45°C decreases significantly and it converts the concentration of dissolved




(a)

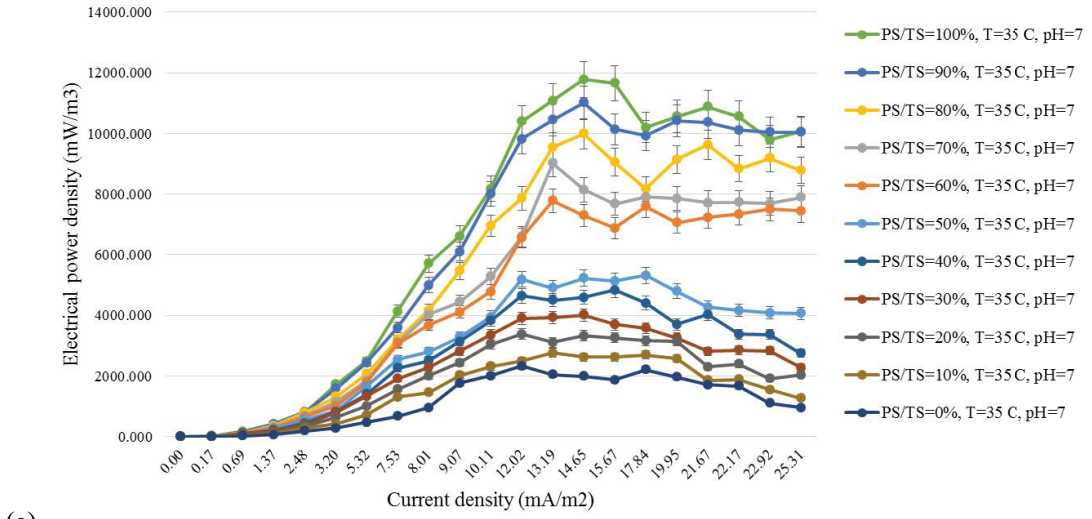



(b)

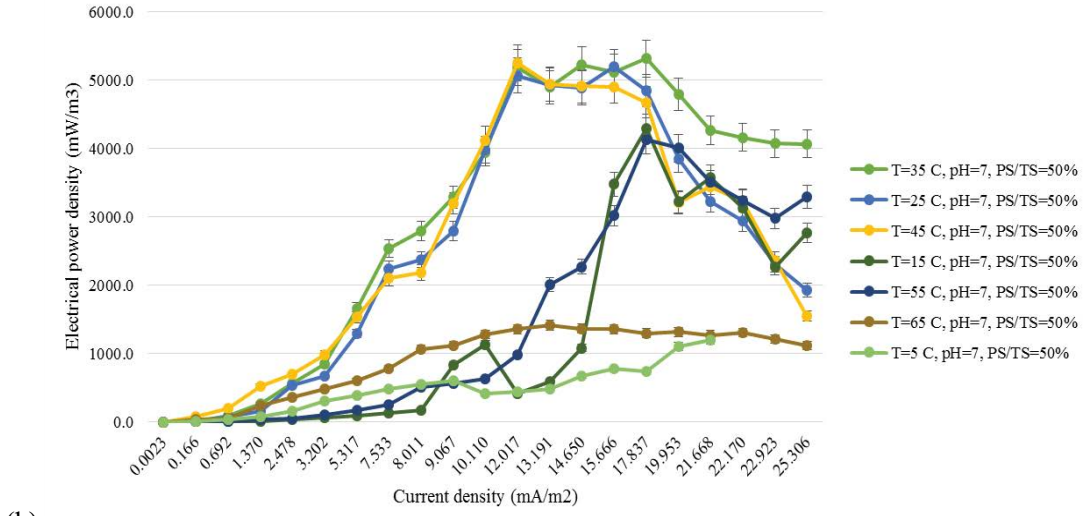



(c)

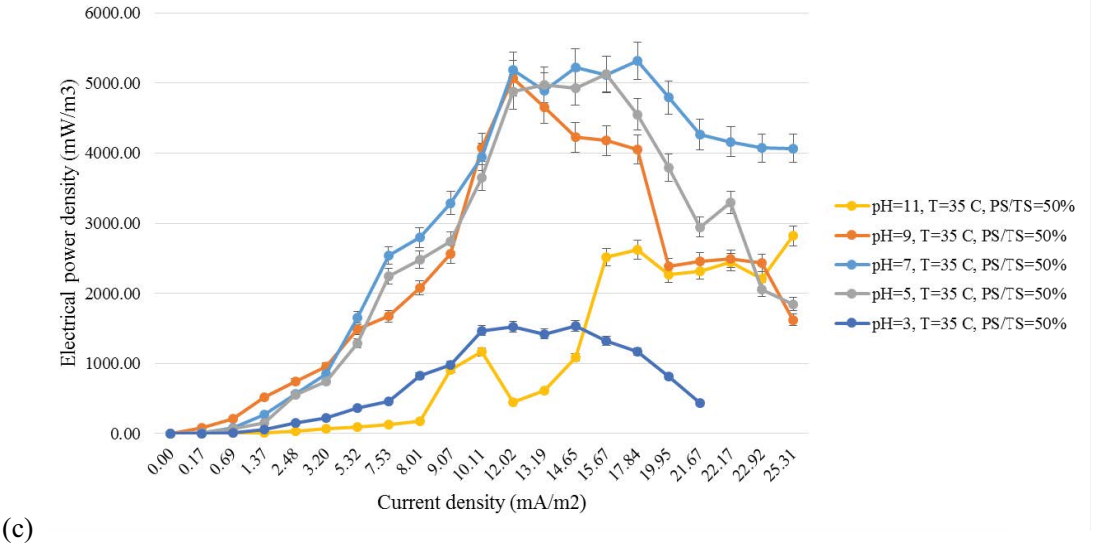
Fig. 8. Polarization curves of the process at various, (a) PS/TS atios, (b) temperatures, and (c) pH values




(a)




(b)




(c)

Fig. 9. Generated electrical power density of the process at various, (a) PS/TS ratios, (b) temperatures, and (c) pH values.

oxygen to the determinant factor of the system's behavior. Moreover, at low temperatures, the biological activity of the reactor decreases, and this issue controls the efficacies of aerobic digestion and electricity generation processes [29,67,79,80]. In this regard, the highest value of generated power density of the reactor is achieved at 35°C. Also, as mentioned before, in very strong acidic or basic conditions, the electrogen's activities and the ion exchange processes are confined and the electricity generation is dropped in these conditions. More species are able to work efficiently in neutral conditions compared with acidic or basic situations, too [70–72,81].

### 3.4. Determination and confirmation of the best performance point

Fig. 10 demonstrates the contour plot which shows the optimized conditions of the reactor, determined through the RSM process. As shown in Fig. 10, the optimized conditions for the reactor performance have been determined 35.87°C, 7.27, and 53.08% for temperature, pH, and primary sludge content of the influent, respectively, and the reactor is expected to remove about 45.81% of the VSS content of the feed sludge and 8,950 mW/m$^3$ electrical power density in these conditions. Also, Fig. 11 shows the situation of the optimized conditions point of each operational parameter and response in their interval.

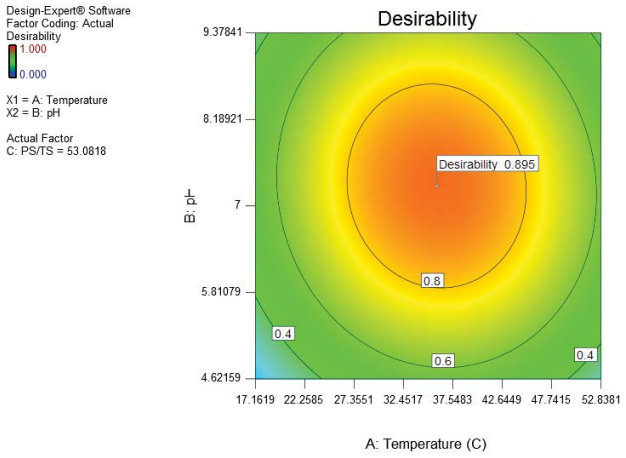



Fig. 10. Contour plot of the integrated optimized conditions of the process considering two responses (the VSS removal efficiency and the generated electrical power density).

According to Fig. 11, the desirability of the optimized conditions is remarkably high (0.895 out of 1) which state the considerably high compatibility of the models for the responses.

In order to confirm the validity of the optimized conditions, an experimental evaluation has been carried out and the results were considerably close to the predicted values (49.65% for the VSS removal efficiency and 8,836 mW/m$^3$ for the maximum generated electrical power density). It means that there is good coverage between the results observed by the experiments and derived from the models. Therefore, it can be derived from various viewpoints that the models are noticeably precise to predict the performance of the reactor and the progress degree of the process in different conditions.

## 4. Conclusions

The optimized conditions for the direct electricity generation process from sewage sludge (containing both primary and secondary sludge), simultaneous with its effective aerobic stabilization process have been determined. The optimization process has been done by RSM and a mathematical correlation between operational conditions of the process and its responses (the VSS removal efficiency and the generated electrical power density), has been developed. Other than the experiments that have been designed by RSM, different experiments have been executed in order to check the validity of the model's results (the values and trends). According to the model's outputs, the optimized conditions for the reactor performance

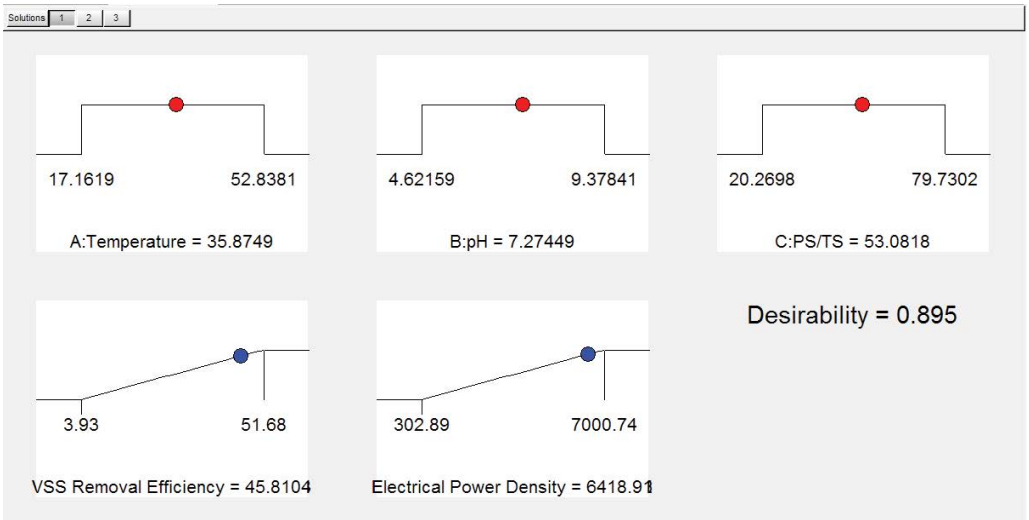



Fig. 11. Situation of the optimized conditions of the process in the interval of each operational parameter and response.

have been determined 35.87°C, 7.27, and 53.08% for temperature, pH, and primary sludge content of the influent, respectively, 45.81% and 8,950 mW/m$^3$ for the VSS removal efficiency and the generated electrical power density. The results of the experiments demonstrated that by increasing the amount of the primary sludge in the influent sludge to the MFC, the VSS removal efficiency decreases, but the generated direct electricity would be modified. Also, the results provided from the experiments and the models confirmed each other with a remarkable accuracy which made the obtained equations of the optimization process valid enough to be considered in process designing and operation. Another approach about the optimization results was that the optimized conditions for stabilization and electricity generation processes covered each other very well.

**Funding**

No grant or financial assistance has been received from funding agencies in the public, commercial, or not-for-profit sectors for carrying out this research.

**References**

[1] B.S. Silvestre, D.M. Ţîrcă, Innovations for sustainable development: moving toward a sustainable future, J. Cleaner Prod., 208 (2019) 325–332.
[2] R.L. Burritt, C. Herzig, S. Schaltegger, T. Viere, Diffusion of environmental management accounting for cleaner production: evidence from some case studies, J. Cleaner Prod., 224 (2019) 479–491.
[3] H. Li, W. Bao, C. Xiu, Y. Zhang, H. Xu, Energy conservation and circular economy in China's process industries, Energy, 35 (2010) 4273–4281.
[4] A.G. Olabi, Circular economy and renewable energy, 181 (2019) 450–454.
[5] Q. Zhu, Y. Geng, K.H. Lai, Circular economy practices among Chinese manufacturers varying in environmental-oriented supply chain cooperation and the performance implications, J. Environ. Manage., 91 (2010) 1324–1331.
[6] S. Tiwari, C.R. Behera, B. Srinivasan, Simulation and experimental studies to enhance water reuse and reclamation in India's largest dairy industry, J. Environ. Chem. Eng., 4 (2016) 605–616.
[7] W. Chen, X. Yin, H. Zhang, Towards low carbon development in China: a comparison of national and global models, J. Clim. Change, 136 (2016) 95–108.
[8] L.E. Borge, P. Parmer, R. Torvik, Local natural resource curse?, J. Public Econ., 131 (2015) 101–114.
[9] G. Venkatesh, R. Abdi Elmi, Economic environmental analysis of handling biogas from sewage sludge digesters in WWTPs (wastewater treatment plants) for energy recovery: case study of Bekkelaget WWTP in Oslo (Norway), J. Energy, 58 (2013) 220–235.
[10] L.P. Lauven, An optimization approach to biorefinery setup planning, Biomass Bioenergy, 70 (2014) 440–451.
[11] V.K. Tyagi, S.L. Lo, Sludge: a waste or renewable source for energy and resources recovery?, J. Renewable Sustainable Energy Rev., 25 (2013) 708–728.
[12] H. Singh, G. Chauhan, A.K. Jain, S.K. Sharma, Adsorptive potential of agricultural wastes for removal of dyes from aqueous solutions, Environ. Chem. Eng., 5 (2017) 122–135.
[13] H.R. Sadabad, G.B. Gholikandi, Experimental study of direct bio-electricity generation from municipal waste-activated sludge simultaneously with its stabilization and modeling the process by KSOFM and MLP artificial neural networks, Desal. Water Treat., 93 (2017) 239–249.
[14] H.R. Sadabad, G.B. Gholikandi, Harvesting direct electricity from municipal waste-activated sludge simultaneous with its aerobic stabilization process: investigation and optimization, J. Environ. Chem. Eng., 5 (2017) 1174–1185.
[15] H.R. Sadabad, G.B. Gholikandi, Simultaneous effective sludge stabilization and direct electricity generation by merging microbial fuel cell (MFC) and Fered-Fenton reactor: an experimental study, Biomass Bioenergy J., 119 (2018) 75–89.
[16] S.H. Joo, F.D. Monaco, E. Antmann, P. Chorath, Sustainable approaches for minimizing biosolids production and maximizing reuse options in sludge management: a review, J. Environ. Manage., 158 (2015) 133–145.
[17] A. Zielinska, P. Oleszczuk, The conversion of sewage sludge into biochar reduces polycyclic aromatic hydrocarbon content and ecotoxicity but increases trace metal content, J. Biomass Bioenergy, 75 (2015) 235–244.
[18] A.C. Sophia, V.M. Bhalambaal, E.C. Lima, M. Thirunavoukkarasu, Microbial desalination cell technology: contribution to sustainable waste water treatment process, current status and future applications, J. Environ. Chem. Eng., 4 (2016) 3468–3478.
[19] Z. Ge, F. Zhang, J. Grimaud, J. Hurst, Z. He, Long-term investigation of microbial fuel cells treating primary sludge or digested sludge, Bioresour. Technol., 136 (2013) 509–514.
[20] N. Mills, P. Pearce, J. Farrow, R.B. Thorpe, N.F. Kirkby, Environmental and economic life cycle assessment of current & future sewage sludge to energy technologies, Waste Manage., 34 (2014) 185–195.
[21] N. Birjandi, H. Younesi, A.A. Ghoreyshi, M. Rahimnejad, Electricity generation through degradation of organic matters in medicinal herbs wastewater using bio-electro-Fenton system, J. Environ. Manage., 180 (2016) 390–400.
[22] A. Hussain, M. Manuel, B. Tartakovsky, A comparison of simultaneous organic carbon and nitrogen removal in microbial fuel cells and microbial electrolysis cells, J. Environ. Manage., 173 (2016) 23–33.
[23] C. Jayashree, K. Tamilarasan, M. Rajkumar, P. Arulazhagan, K.N. Yogalakshmi, M. Srikanth, J.R. Banu, Treatment of seafood processing wastewater using upflow microbial fuel cell for power generation and identification of bacterial community in anodic biofilm, J. Environ. Manage., 180 (2016) 351–358.
[24] J. Choi, Y. Ahn, Increased power generation from primary sludge in microbial fuel cells coupled with prefermentation, Bioprocess. Biosyst. Eng., 37 (2014) 2549–2557.
[25] D. Pant, G. Van Bogaert, L. Diels, K. Vanbroekhoven, A review of the substrates used in microbial fuel cells (MFCs) for sustainable energy production, Bioresour. Technol., 101 (2010) 1533–1543.
[26] H. Wang, J.D. Park, Z. Ren, Active energy harvesting from microbial fuel cells at the maximum power point without using resistors, Environ. Sci. Technol., 46 (2012) 5247–5252.
[27] H. Ren, H.S. Lee, J. Chae, Miniaturizing microbial fuel cells for potential portable power sources: promises and challenges, Microfluid. Nanofluid., 13 (2012) 353–381.
[28] U. Karra, S.S. Manickam, J.R. McCutcheon, N. Patel, B. Li, Power generation and organics removal from wastewater using activated carbon nanofiber (ACNF) microbial fuel cells (MFCs), Int. J. Hydrogen Energy, 38 (2013) 1588–1597.
[29] S. Cheng, P. Kiely, B.E. Logan, Pre-acclimation of a wastewater inoculum to cellulose in an aqueous–cathode MEC improves power generation in air–cathode MFCs, Bioresour. Technol., 102 (2011) 367–371.
[30] I. Shizas, D.M. Bagley, Experimental determination of energy content of unknown organics in municipal wastewater streams, J. Energy Eng., 130 (2004) 45–53.
[31] A.V. Schenone, L.O. Conte, M.A. Botta, O.M. Alfano, Modeling and optimization of photo-Fenton degradation of 2,4-D using ferrioxalate complex and response surface methodology (RSM), J. Environ. Manage., 155 (2015) 177–183.
[32] S. Ghafari, H.A. Aziz, M.H. Isa, A.A. Zinatizadeh, Application of response surface methodology (RSM) to optimize coagulation–flocculation treatment of leachate using poly-aluminum chloride (PAC) and alum, J. Hazard. Mater., 163 (2009) 650–656.
[33] S.S. Moghaddam, M.A. Moghaddam, M. Arami, Coagulation/flocculation process for dye removal using sludge from water

treatment plant: optimization through response surface methodology, J. Hazard. Mater., 175 (2010) 651–657.
[34] C.M. Borror, D.C. Montgomery, R.H. Myers, Evaluation of statistical designs for experiments involving noise variables, J. Qual. Technol., 34 (2002) 54–70.
[35] U.T. Un, A. Kandemir, N. Erginel, S.E. Ocal, Continuous electrocoagulation of cheese whey wastewater: an application of response surface methodology, J. Environ. Manage., 146 (2014) 245–250.
[36] G. Guven, A. Perendeci, A. Tanyolac, Electrochemical treatment of deproteinated whey wastewater and optimization of treatment conditions with response surface methodology, J. Hazard. Mater., 157 (2008) 69–78.
[37] D. Hou, R. Goei, X. Wang, P. Wang, T.T. Lim, Preparation of carbon-sensitized and Fe–Er codoped $TiO_2$ with response surface methodology for bisphenol A photocatalytic degradation under visible-light irradiation, Appl. Catal., B, 126 (2012) 121–133.
[38] APHA, Standard Methods for Examination of Water and Wastewaters, 20th ed., U.S. Environmental Protection Agency, American Public Health Association, Washington, DC, 1999.
[39] L. Metcalf, H.P. Eddy, G. Tchobanoglous, Wastewater Engineering: Treatment, Disposal, and Reuse, McGraw-Hill, New York, NY, 2010.
[40] J. Jiang, Q. Zhao, J. Zhang, G. Zhang, D.J. Lee, Electricity generation from bio-treatment of sewage sludge with microbial fuel cell, Bioresour. Technol., 100 (2009) 5808–5812.
[41] M. Hosseinpour, M. Vossoughi, I. Alemzadeh, An efficient approach to cathode operational parameters optimization for microbial fuel cell using response surface methodology, J. Environ. Health Sci. Eng., 12 (2014) 1–11.
[42] B. Min, O.B. Roman, I. Angelidaki, Importance of temperature and anodic medium composition on microbial fuel cell (MFC) performance, Biotechnol. Lett., 30 (2008) 1213–1218.
[43] H. Liu, S. Cheng, B.E. Logan, Power generation in fed-batch microbial fuel cells as a function of ionic strength, temperature, and reactor configuration, Environ. Sci. Technol., 39 (2005) 5488–5493.
[44] J.C. Biffinger, J. Pietron, O. Bretschger, L.J. Nadeau, G.R. Johnson, C.C. Williams, B.R. Ringeisen, The influence of acidity on microbial fuel cells containing *Shewanella oneidensis*, Biosens. Bioelectron., 24 (2008) 900–905.
[45] G.S. Jadhav, M.M. Ghangrekar, Performance of microbial fuel cell subjected to variation in pH, temperature, external load and substrate concentration, Bioresour. Technol., 100 (2009) 717–723.
[46] E. Martin, O. Savadogo, S.R. Guiot, B. Tartakovsky, The influence of operational conditions on the performance of a microbial fuel cell seeded with mesophilic anaerobic sludge, Biochem. Eng. J., 51 (2010) 132–139.
[47] V. Vologni, R. Kakarla, I. Angelidaki, B. Min, Increased power generation from primary sludge by a submersible microbial fuel cell and optimum operational conditions, Bioprocess. Biosyst. Eng., 36 (2013) 635–642.
[48] A. Larrosa-Guerrero, K. Scott, K.P. Katuri, C. Godinez, I.M. Head, T. Curtis, Open circuit versus closed circuit enrichment of anodic biofilms in MFC: effect on performance and anodic communities, Appl. Microbiol. Biotechnol., 87 (2010) 1699–1713.
[49] S. Puig, M. Serra, M. Coma, M. Cabré, M.D. Balaguer, J. Colprim, Effect of pH on nutrient dynamics and electricity production using microbial fuel cells, Bioresour. Technol., 101 (2010) 9594–9599.
[50] T. Zhang, C. Cui, S. Chen, H. Yang, P. Shen, The direct electrocatalysis of *Escherichia coli* through electro-activated excretion in microbial fuel cell, Electrochem. Commun., 10 (2008) 293–297.
[51] F. Yang, L. Ren, Y. Pu, B.E. Logan, Electricity generation from fermentation solution of primary sludge using single-chambered air-cathode microbial fuel cells, Bioresour. Technol., 128 (2013) 784–787.
[52] G.D. Zupancic, M. Ros, Aerobic and two-stage anaerobic–aerobic sludge digestion with pure oxygen and air aeration, Bioresour. Technol., 99 (2008) 100–109.
[53] W.J. Jewell, R.M. Kabrick, Autoheated aerobic thermophilic digestion with aeration, J. Water Pollut. Control Fed., (1980) 512–523.
[54] G.C. Gil, I.S. Chang, B.H. Kim, M. Kim, J.K. Jang, H.S. Park, H.J. Kim, Operational parameters affecting the performannce of a mediator-less microbial fuel cell, Biosens. Bioelectron., 18 (2003) 327–334.
[55] J. Guo, Y. Peng, S. Wang, Y. Zheng, H. Huang, Z. Wang, Long-term effect of dissolved oxygen on partial nitrification performance and microbial community structure, Bioresour. Technol., 100 (2009) 2796–2802.
[56] S. Hawash, N. El-Ibiari, F.H. Aly, G. El-Diwani, M.A. Hamad, Kinetic study of thermophilic aerobic stabilization of sludge, Biomass Bioenergy, 6 (1994) 283–286.
[57] J.O. Ugwuanyi, L.M. Harvey, B. McNeil, Effect of digestion temperature and pH on treatment efficiency and evolution of volatile fatty acids during thermophilic aerobic digestion of model high strength agricultural waste, Bioresour. Technol., 96 (2005) 707–719.
[58] S. Bernard, N.F. Gray, Aerobic digestion of pharmaceutical and domestic wastewater sludges at ambient temperature, Water Res., 34 (2000) 725–734.
[59] S. Oh, B. Min, B.E. Logan, Cathode performance as a factor in electricity generation in microbial fuel cells, Environ. Sci. Technol., 38 (2004) 4900–4904.
[60] Y. Fan, H. Hu, H. Liu, Enhanced Coulombic efficiency and power density of air-cathode microbial fuel cells with an improved cell configuration, J. Power Sources, 171 (2007) 348–354.
[61] U. Schroder, J. Nieben, F. Scholz, A generation of microbial fuel cells with current outputs boosted by more than one order of magnitude, Angew. Chem. Int. Ed., 42 (2003) 2880–2883.
[62] R.A. Rozendal, H.V. Hamelers, C.J. Buisman, Effects of membrane cation transport on pH and microbial fuel cell performance, Environ. Sci. Technol., 40 (2006) 5206–5211.
[63] A. El-Mekawy, H.M. Hegab, X. Dominguez-Benetton, D. Pant, Internal resistance of microfluidic microbial fuel cell: challenges and potential opportunities, Bioresour. Technol., 142 (2013) 672–682.
[64] B.H. Kim, I.S. Chang, G.M. Gadd, Challenges in microbial fuel cell development and operation, Appl. Microbiol. Biotechnol., 76 (2007) 485–494.
[65] B.E. Logan, J.M. Regan, Electricity-producing bacterial communities in microbial fuel cells, Trends Microbiol., 14 (2006) 512–518.
[66] T.D. Brock, Thermophilic Microorganisms and Life at High Temperatures, Springer Science & Business Media, New York, NY, 2012.
[67] N. Beales, Adaptation of microorganisms to cold temperatures, weak acid preservatives, low pH, and osmotic stress: a review, Compr. Rev. Food Sci. Food Saf., 3 (2004) 1–20.
[68] R. Margesin, J. Cimadom, F. Schinner, Biological activity during composting of sewage sludge at low temperatures, Int. Biodeterior. Biodegrad., 57 (2006) 88–92.
[69] H. Liu, B.E. Logan, Electricity generation using an air-cathode single chamber microbial fuel cell in the presence and absence of a proton exchange membrane, Environ. Sci. Technol., 38 (2004) 4040–4046.
[70] Z. He, Y. Huang, A.K. Manohar, F. Mansfeld, Effect of electrolyte pH on the rate of the anodic and cathodic reactions in an air-cathode microbial fuel cell, Bioelectrochemistry, 74 (2008) 78–82.
[71] H.N. Gavala, U. Yenal, I.V. Skiadas, P. Westermann, B.K. Ahring, Mesophilic and thermophilic anaerobic digestion of primary and secondary sludge. Effect of pre-treatment at elevated temperature, Water Res., 37 (2003) 4561–4572.
[72] H.A. Painter, J.E. Loveless, Effect of temperature and pH value on the growth-rate constants of nitrifying bacteria in the activated-sludge process, Water Res., 17 (1983) 237–248.
[73] K. Belafi-Bako, B. Vajda, N. Nemestothy, Study on operation of a microbial fuel cell using mesophilic anaerobic sludge, Desal. Water Treat., 35 (2011) 222–226.
[74] Z. He, J. Kan, Y. Wang, Y. Huang, F. Mansfeld, K.H. Nealson, Electricity production coupled to ammonium in a microbial fuel cell, Environ. Sci. Technol., 43 (2009) 3391–3397.

[75] Z. He, N. Wagner, S.D. Minteer, L.T. Angenent, An upflow microbial fuel cell with an interior cathode: assessment of the internal resistance by impedance spectroscopy, Environ. Sci. Technol., 40 (2006) 5212–5217.
[76] Y. Fan, E. Sharbrough, H. Liu, Quantification of the internal resistance distribution of microbial fuel cells, Environ. Sci. Technol., 42 (2008) 8101–8107.
[77] P. Liang, X. Huang, M.Z. Fan, X.X. Cao, C. Wang, Composition and distribution of internal resistance in three types of microbial fuel cells, Appl. Microbiol. Biotechnol., 77 (2007) 551–558.
[78] P.Y. Zhang, Z.L. Liu, Experimental study of the microbial fuel cell internal resistance, J. Power Sources, 195 (2010) 8013–8018.
[79] B. Erable, N. Duteanu, S.S. Kumar, Y. Feng, M.M. Ghangrekar, K. Scott, Nitric acid activation of graphite granules to increase the performance of the non-catalyzed oxygen reduction reaction (ORR) for MFC applications, Electrochem. Commun., 11 (2009) 1547–1549.
[80] S.E. Oh, J.R. Kim, J.H. Joo, B.E. Logan, Effects of applied voltages and dissolved oxygen on sustained power generation by microbial fuel cells, Water Sci. Technol., 60 (2009) 1311–1317.
[81] B.M. Wilen, J.L. Nielsen, K. Keiding, P.H. Nielsen, Influence of microbial activity on the stability of activated sludge flocs, Colloids Surf., B, 18 (2000) 145–156.